Solitary Pulmonary Nodule: Characterization with Combined Wash-in and Washout Features at Dynamic Multi–Detector Row CT[1]

Yeon Joo Jeong, MD[2]
Kyung Soo Lee, MD
Sun Young Jeong, MD
Myung Jin Chung, MD
Sung Shine Shim, MD
Hojoong Kim, MD
O Jung Kwon, MD
Seonwoo Kim, PhD

Published online
10.1148/radiol.2372041549
Radiology 2005; 237:675–683

[1] From the Department of Radiology and Center for Imaging Science (Y.J.J., K.S.L., S.S.S., S.Y.J., M.J.C.), Division of Pulmonary and Critical Care Medicine, Department of Medicine (H.K., O.J.K.), and Biostatistics Unit (S.K.), Samsung Medical Center, Sungkyunkwan University School of Medicine, 50 Ilwon-Dong, Kangnam-Ku, Seoul 135-710, Korea. Received September 8, 2004; revision requested November 12; revision received November 19; accepted December 30. **Address correspondence to** K.S.L. (e-mail: *kyungs.lee@samsung.com*).

Authors stated no financial relationship to disclose.

Current address:
[2] Department of Radiology, Pusan National University Hospital, Pusan, Korea.

Author contributions:
Guarantor of integrity of entire study, K.S.L.; study concepts/study design or data acquisition or data analysis/interpretation, all authors; manuscript drafting or manuscript revision for important intellectual content, all authors; approval of final version of submitted manuscript, all authors; literature research, Y.J.J., K.S.L., H.K., O.J.K.; clinical studies, Y.J.J., S.Y.J., M.J.C., S.S.S.; statistical analysis, Y.J.J., K.S.L., S.W.K.; and manuscript editing, Y.J.J., K.S.L., M.J.C., S.S.S., O.J.K.

PURPOSE: To prospectively assess the accuracy of combined wash-in and washout characteristics at dynamic contrast material–enhanced multi–detector row computed tomography (CT) in distinguishing benign from malignant solitary pulmonary nodules.

MATERIALS AND METHODS: Institutional review board approval and informed consent were obtained. The study included 107 patients (62 men, 45 women; mean age, 55 years; range, 22–81 years) with a solitary pulmonary nodule. After unenhanced CT (2.5-mm collimation) scans were obtained, dynamic CT was performed by using a helical technique (series of images obtained throughout the nodule, with 2.5-mm collimation, at 30, 60, 90, and 120 seconds and 4, 5, 9, 12, and 15 minutes) after intravenous injection of contrast medium (120 mL). Tissue diagnosis was made in 70 nodules, and follow-up images showed benignancy in the remaining 37 (no change in size, $n = 32$; decrease in size, $n = 5$). CT findings were analyzed in terms of wash-in and washout of contrast medium. Sensitivity, specificity, and accuracy for malignant nodules were calculated by considering both the wash-in and washout characteristics at dynamic CT.

RESULTS: There were 49 malignant and 58 benign nodules. When diagnostic criteria for malignancy of both wash-in of 25 HU or greater and washout of 5–31 HU were applied, sensitivity, specificity, and accuracy for malignancy were 94% (46 of 49 nodules), 90% (52 of 58 nodules), and 92% (98 of 107 nodules), respectively. Of 58 benign nodules, 27 showed less than 25 HU wash-in, 14 showed persistent contrast enhancement without washout and with wash-in of 25 HU or greater, and 11 showed washout greater than 31 HU and wash-in of 25 HU or greater.

CONCLUSION: Evaluation of solitary pulmonary nodules by analyzing combined wash-in and washout characteristics at dynamic contrast-enhanced multi–detector row CT showed 92% accuracy for distinguishing benign nodules from malignant nodules.

Computed tomography (CT) is the modality of choice in the imaging characterization of pulmonary nodules. The evaluation of tumor vascularity by using contrast material–enhanced CT has proved to be useful for differentiating between malignant and benign nodules (1–4). Various threshold attenuation values have been reported to be useful for distinguishing malignant nodules from benign nodules at contrast-enhanced dynamic CT with single– or multi–detector row helical machines (1,2,4–6). In general, malignant nodules tend to enhance substantially more than do benign nodules (1,2,4–7). However, in previous studies, which were focused on the early phase of dynamic CT scanning, some overlap was found between malignant nodules and benign nodules, for example, active

granulomas or benign vascular tumors (4,7). Therefore, although results of these dynamic studies showed high sensitivity for the diagnosis of malignant nodules, the specificity was too low. In addition, approximately 50% of indeterminate lung nodules, for which diagnosis is obtained at surgery, are benign, and hospitalization for the surgical removal of these nodules is expensive and involves a certain extent of morbidity and mortality (8–12). Therefore, the need for noninvasive imaging modalities for the specific diagnosis of indeterminate lung nodules has been raised.

More recently, several authors have attempted to assess the washout characteristics of adrenal lesions at contrast-enhanced CT (13–17). Washout refers to the reduction in the attenuation values of lesions at CT during a variable period after the intravenous injection of a bolus of contrast material. Many study findings now confirm the usefulness of attenuation measurements at both unenhanced and delayed contrast-enhanced CT for the differentiation of benign from malignant adrenal lesions (13–17).

To the best of our knowledge, no evaluation of the accuracy of pulmonary nodule washout characterization at dynamic contrast-enhanced CT has been reported. The purpose of our study was to prospectively assess the accuracy of combined wash-in and washout characteristics with dynamic contrast-enhanced multi–detector row CT in distinguishing benign from malignant solitary pulmonary nodules.

MATERIALS AND METHODS

Patients and CT Imaging

From October 2003 to June 2004, a total of 155 patients (95 men and 60 women; age range, 22–90 years; mean age, 54 years) with a solitary pulmonary nodule (<3 cm in longest diameter, approximately spherical; short- and long-axis diameters were within a factor of 1.5 of each other) at chest radiography underwent dynamic chest CT. These CT examinations were performed by using a four–detector row (LightSpeed QX/i; GE Medical Systems, Milwaukee, Wis) or 16–detector row (LightSpeed Ultra or Ultra16; GE Medical Systems) scanner. Our institutional review board approved our research protocol for this CT study, and written informed consent was obtained from all patients.

Before dynamic CT was performed, we obtained targeted thin-section helical CT scans (2.5-mm collimation, 0.8-second gantry rotation time, 120 kVp, 90 mA) through the nodule. Nodules that appeared to be solitary at chest radiography but appeared to have a satellite nodule at thin-section CT ($n = 22$) were included in this study. For those nodules with a satellite lesion, only the main nodule was evaluated with dynamic contrast-enhanced CT. Nodules were excluded from study if they had benign (diffuse, laminated, popcornlike, or central) patterns of calcification ($n = 17$) or fat ($n = 0$) at thin-section CT. Nodules with ground-glass opacity at thin-section CT were also excluded ($n = 7$). Nodules with stippled ($n = 3$) or peripheral nodular ($n = 12$) calcification were included. Dynamic CT was performed in the remaining 131 patients.

Before the intravenous injection of contrast medium, a series of 13 images was obtained throughout the nodule for 30 mm along the z-axis, with 2.5-mm collimation, 120 kVp, 90 mA, 0.8-second gantry rotation time, and a table speed of 3.75 mm/sec over 8 seconds. Thereafter, an additional nine series of images were obtained at 30, 60, 90, and 120 seconds and 4, 5, 9, 12, and 15 minutes after injection of iomeprol (Iomeron 300; Bracco, Milan, Italy), which was administered at a rate of 3 mL/sec for a total of 120 mL by using a power injector (MCT Plus; Medrad, Pittsburgh, Pa), with the same parameters as used for the initial preenhancement series (10 total series of images obtained at 0, 30, 60, 90, and 120 seconds and 4, 5, 9, 12, and 15 minutes). Image data were reconstructed with a thickness of 2.5 mm (13 images in each cluster; total number of dynamic images, 130 [ie, 13 images × 10 series]) by using a standard algorithm. Immediately after dynamic imaging at 120 seconds, helical CT scans (125 mA, 120 kVp, 5-mm collimation, table speed of 15 mm/sec) were obtained from the lung apices to the level of the middle pole of both kidneys for tumor staging. All thin-section, dynamic, and staging CT data were interfaced directly to our picture archiving and communication system (Centricity 1.0; GE Medical Systems Integrated Imaging Solutions, Mt Prospect, Ill), which displayed all image data on monitors (four monitors, 1536 × 2048 image matrices, 8-bit viewable gray scale, 60-foot-lambert luminescence). On the monitors, both mediastinal window (width, 400 HU; level, 20 HU) and lung window (width, 1500 HU; level, −700 HU) images were viewed.

The technical adequacy of dynamic CT fulfilled the following criteria, as presented in previous studies (2,6): *(a)* absence of contrast medium extravasation at the site of injection, *(b)* appropriate enhancement of cardiovascular structures imaged during examination, *(c)* no marked reaction to contrast medium that interfered with image acquisition, and *(d)* satisfactory patient respiratory registration without artifact on equatorial images. In four patients, inconsistent breath holding was a problem for obtaining dynamic image clusters at the same level. In another 10 patients, the nodules were too small (<5.6 mm in diameter) to measure the attenuation value (partial volume averaging precluded the measurement of attenuation value). With the exception of these 14 patients, the dynamic CT scans were technically adequate in 117 patients, and no serious reactions to contrast medium were reported. No CT examination was interrupted because of reaction to contrast medium.

Of 117 patients, 10 were excluded because neither follow-up CT scans nor cytologic or histologic diagnosis was available for these patients. Therefore, the final study group was 107 patients, which comprised 62 men and 45 women aged 22–81 years (mean, 55 years). The body weight of these 107 patients ranged from 36 to 90 kg (mean, 64 kg; standard deviation, ±10 kg). These patients underwent transthoracic needle biopsy ($n = 39$) or surgery ($n = 31$), which included lobectomy ($n = 20$) or wedge resection ($n = 11$). Thirty-seven patients in whom CT findings and clinical situations suggested benignancy of a nodule but histopathologic diagnosis was not obtained were regarded to have a benign nodule because the nodules did not change in diameter ($n = 32$) or decreased in diameter ($n = 5$). Nodules that did not change in size were followed up with CT at least once or more than once over 9–14 months (mean, 11.7 months; standard deviation, ±1.3 months).

Radiation Exposure

Radiation exposure was determined by means of thermoluminescent dosimetry, as described by Jung et al (18). Total organ doses of thin-section, dynamic, and staging CT studies were calculated. Four lithium fluoride chips were placed in the bilateral upper and lower lung zones of the irradiated lungs of a phantom: one in the right upper lung zone, one in the left upper lung zone, one in the right lower lung zone, and one in the left lower lung zone. Radiation doses were measured

TABLE 1
Diagnoses of 107 Nodules

Nodule Type and Diagnosis	No. of Nodules
Malignant	49 (46)
Adenocarcinoma	33
Non–small cell lung cancer	8
Squamous cell carcinoma	3
Bronchioloalveolar cell carcinoma	1
Small cell carcinoma	1
Pleomorphic carcinoma	1
Carcinoid tumor	1
Metastatic carcinoma	1
Benign	58 (54)
Follow-up with imaging	37
Hamartoma	8
Focal pneumonia without specific microorganism	4
Tuberculosis	2
Pulmonary infiltration of eosinophilia	2
Sclerosing hemangioma	1
Aspergilloma	1
Anthracofibrosis	1
Progressive massive fibrosis	1
Leiomyoma	1

Note.—Data in parentheses are percentages.

twice: once with the presumption that the nodule was located in the upper lung zone and once with the presumption that the nodule was located in the lower lung zone. The radiation doses (at nodule sites and at other lung sites away from the nodule locations) were calculated by measuring the doses absorbed by the lithium fluoride chips placed inside the phantom. The measured organ dose was compared with that at standard thoracic helical CT (beam collimation of 20 mm, beam pitch of 0.75, 0.8-second rotation time, 120 kVp, and 210 mA) at our institution.

Evaluation of Morphologic Features at Targeted Thin-Section CT

One radiologist (K.S.L.) with 14 years of experience in chest CT evaluated the morphologic features. Morphologic features of nodules, including margins, presence or absence of a satellite lesion, and cavity were assessed. Nodule margins were classified as smooth, lobulated, or spiculated. Long-axis diameters of the nodules were also measured on images with lung window settings.

Evaluation of Enhancement Dynamics

After viewing all 130 images as thumbnail images on a picture archiving and communications monitor, we selected one image for analysis from the 13 images obtained at each time point. The selected image was the transverse section with the largest diameter (scanned at the equator of the nodule). We measured attenuation values of the nodules in the same area on the selected image for each cluster at each time point (ie, from the unenhanced image to the image acquired at 15 minutes). A circular region of interest was placed over the nodule. We examined a region of interest that covered about one-half of the diameter of the nodule at the equator. When we were confronted with areas that were calcified ($n = 8$; average area at the selected image, 5%; range, 2%–20%), cavitary ($n = 9$; average area, 24%; range, 2%–40%), or necrotic ($n = 22$; average area, 17%; range, 5%–60%), these areas were avoided so that the region of interest was made as large as possible away from these areas. All Hounsfield unit measurements were performed by using mediastinal window images to ensure that partial volume averaging was minimized.

Two radiologists (Y.J.J. and K.S.L., with 2 and 14 years of experience in chest CT, respectively) measured the attenuation values independently. All measurements were obtained at the time of the CT examination, and the radiologists were blinded to features, including patients' age and clinical history, that might influence their CT measurements. Two measurements were obtained for each nodule at each imaging phase by each observer. Each observer recorded the mean attenuation values and then analyzed and calculated the following dynamic characteristics of tumor enhancement by using wash-in and washout values of the contrast medium: peak enhancement, net enhancement (wash-in), and absolute and relative loss of enhancement (washout). Peak enhancement was defined as the maximum attenuation value of the nodule over the entire duration of the dynamic study. Net enhancement was calculated by subtracting the preenhancement attenuation value from the peak enhancement attenuation value. Absolute loss of enhancement at delayed imaging was calculated by subtracting the attenuation value at 15 minutes (AT_{15}) from the peak enhancement attenuation value (AT_{peak}). The relative percentage loss of enhancement was calculated as follows: $[(AT_{peak} - AT_{15})/AT_{peak}] \cdot 100$.

Data and Statistical Analyses

Statistical analyses were performed by using commercially available software (SAS 8.2; SAS Institute, Cary, NC). Agreement in measured attenuation values of nodules between the two observers was analyzed by calculating the intraclass correlation coefficient.

A retrospective calculation was used to evaluate the usefulness of net enhancement as a marker for malignant nodules (vs benign nodules) at early-phase dynamic CT. Sensitivity, specificity, accuracy, and positive and negative predictive values were calculated by varying the level of enhancement that signified a positive finding (cutoff value).

Washout was also calculated retrospectively at different cutoff levels to differentiate malignant nodules from benign nodules during the delayed phase of dynamic CT.

Diagnostic characteristics—that is, sensitivity, specificity, accuracy, positive predictive value, and negative predictive value—were calculated by considering both the wash-in (net enhancement) and washout (absolute loss of enhancement) characteristics at dynamic CT.

The χ^2 test, Fisher exact test, Student t test, and Mann-Whitney test were used to analyze statistically significant differences between morphologic features and attenuation values for unenhanced imaging, net enhancement, and absolute and relative loss of enhancement in malignant and benign nodules. $P < .05$ was considered to indicate a significant difference.

Multivariate analysis was performed by using the multiple logistic regression method to see how the morphologic characteristics and dynamic enhancement CT results were useful independently from each other in distinguishing between malignant and benign nodules. In other words, we investigated whether a factor of morphologic characteristics and dynamic CT results was related to the outcome variable (malignancy), adjusting the effect of the other factor in the model.

RESULTS

Radiation Exposure

The measured total organ dose at thin-section, dynamic, and staging CT ranged from 98 to 115 mGy at the nodule sites and ranged from 35 to 40 mGy elsewhere in the lungs. The organ dose administered for a standard thoracic helical CT examination at our institution ranges from 39 to 40 mGy.

Unenhanced Targeted Thin-Section CT

Of 107 nodules, 49 (46%) proved to be malignant and 58 (54%) proved to be benign (Table 1). One bronchial carcinoid tumor was classified as malignant. The sizes (in diameter) of the 107 nodules were as follows: In 11 patients, nodules were 5.6 mm or larger but were smaller than 10 mm; in 28 patients, nodules were 10 mm or larger but were smaller than 15 mm; in 32 patients, nodules were 15 mm or larger but were smaller than 20 mm; in 15 patients, nodules were 20 mm or larger but were smaller than 25 mm; and in 21 patients, nodules were 25 mm or larger but were smaller than 30 mm. Malignant nodules were significantly larger (mean diameter, 20.4 mm ± 6.1 [standard deviation]; range, 8.3–30.0 mm) than benign nodules (mean diameter, 16.2 mm ± 6.5; range, 5.6–30.0 mm) ($P = .001$, Student t test). Lobulated margins ($P < .001$, χ^2 test) and spiculated margins ($P < .001$, χ^2 test) were more frequently observed than were smooth margins in malignant nodules. Calcification (two of 49 malignant nodules [4%] vs 13 of 58 benign nodules [22%], $P = .007$) or satellite lesions (three of 49 malignant nodules [6%] vs 18 of 58 benign nodules [31%], $P = .001$, χ^2 test) were more frequently seen in benign nodules.

TABLE 2
Nodule Characteristics at Early Enhancement CT

Characteristic	Malignant Nodules ($n = 49$)	Benign Nodules ($n = 58$)	P Value
Preenhancement value (HU)			
Mean ± SD	47 ± 7.0	44 ± 11.8	.141*
Median	46.0	43.5	
Range	32–62	14–84	
Peak enhancement value (HU)			
Mean ± SD	96 ± 18.7	78 ± 33.6	<.001†
Median	93.0	65.5	
Range	67–146	37–166	
Net enhancement value (HU)			
Mean ± SD	50 ± 16.7	34 ± 31.4	<.001†
Median	48.0	26	
Range	26–90	0–134	
Time to peak enhancement (min)			
Mean ± SD	3.2 ± 2.7	6.4 ± 5.8	.043†
Median	2.0	4.5	
Range	0.5–15	0–15	

Note.—SD = standard deviation.
* Student t test.
† Mann-Whitney test.

Early Enhancement CT and Wash-in of Contrast Material

Good interobserver agreement was obtained in terms of measuring the attenuation values of nodules (intraclass correlation coefficient, 0.879–0.974; $P < .001$).

The characteristics of the enhancement dynamics of nodules on early-phase contrast-enhanced CT are summarized in Table 2. The mean attenuation value for the 58 benign nodules on unenhanced CT scans was 44 HU ± 11.8 (range, 14–84 HU), whereas that for the 49 malignant nodules was 47 HU ± 7.0 (range, 32–62 HU). The mean attenuation value of benign nodules on unenhanced CT scans was not significantly different from that of malignant nodules ($P = .141$).

In 45 of the 49 malignant nodules, peak level of enhancement occurred within 5 minutes of the initiation of contrast material injection. However, in four malignant nodules, peak level of enhancement occurred more than 5 minutes after injection (9 minutes in three nodules, 15 minutes in one nodule; all four were adenocarcinomas) (Table 2). The amount of time to peak enhancement for the 58 benign nodules was widely distributed (within 5 minutes in 35 nodules, after 5 minutes in 23 nodules). Significantly higher peak enhancement was seen in malignant nodules (mean, 96 HU; range, 67–146 HU) than in benign nodules (mean, 78 HU; range, 37–166 HU) ($P < .001$). Therefore, the net enhancement for malignant nodules (mean, 50 HU; range, 26–90 HU) was significantly greater than that for benign nodules (mean, 34 HU; range, 0–134 HU) ($P < .001$). When 25 HU was used as the threshold for a positive finding (ie, net enhancement greater than 25 HU indicates malignancy), the following diagnostic characteristics were obtained: sensitivity of 100%, specificity of 48%, positive predictive value of 62%, negative predictive value of 100%, and accuracy of 72%. False-positive results on early-phase CT scans were obtained in 30 (52%) of 58 benign nodules.

Delayed Enhancement CT and Washout of Contrast Material

Malignant nodules showed greater washout of contrast enhancement (15 HU ± 7.3; range of 0–34 HU in absolute loss or 15% ± 6.0 in relative loss) than did benign nodules (14 HU ± 19.9; range of 0–90 HU in absolute loss or 14% ± 14.8 in relative loss) ($P < .001$ and .035, respectively; Mann-Whitney test). Considering the nodule dynamics of both early and delayed enhancement CT, several diagnostic rates were retrospectively calculated at different cutoff values (Table 3). Considering the nodule dynamics of both early and delayed enhancement CT, four kinds of enhancement pattern were observed (Tables 4, 5; Fig 1). Most malignant nodules (46 of 49, 94%) showed more than 25 HU wash-in and 5–31 HU washout of contrast medium (Fig 2). Of 58 benign nodules, 27 showed less than 25 HU wash-in (Fig 3), 14 showed persistent enhancement without washout and with more than 25 HU wash-in (Fig 4), and 11 showed more than 31 HU washout and more than 25 HU wash-in (Fig 5, Table 4).

When diagnostic criteria for malignancy of more than 25 HU wash-in and 5–31 HU washout were applied, sensitivity, specificity, accuracy, positive predictive value, and negative predictive value for malignant nodules were 94%, 90%, 92%, 88%, and 95%, respectively (Table 3). False-positive results were obtained for focal pneumonias without a specific microorganism (three of four nodules, 75%), anthracofibrotic nodule (one of one nodule, 100%), and other unspecified nodules (two of 37 nodules, 5%). False-negative results were obtained for adenocarcinoma of the lung (three of 33 nodules, 9%).

Each of the diagnostic criteria for malignancy—fulfilling both more than 25 HU wash-in and 5–31 HU washout ($P < .001$; odds ratio, 25.7), lobulated margin ($P = .011$; odds ratio, 41.7), spiculated margin ($P = .006$; odds ratio, 35.3), and absence of satellite nodule ($P = .004$;

TABLE 3
Diagnostic Rates of Dynamic Enhancement CT according to Various Thresholds of Cutoff Values

Threshold Values Used (HU)	Sensitivity (%)	Specificity (%)	Accuracy (%)	Positive Predictive Value (%)	Negative Predictive Value (%)
≥25 Wash-in, 5–31 washout	94	90	92	88	95
≥25 Wash-in, 5–33 washout	96	88	92	87	96
≥25 Wash-in, 5–34 washout	98	86	92	86	98

TABLE 4
Patterns of Nodule Enhancement at Early and Delayed Enhancement CT

Pattern of Enhancement (HU)	No. of Malignant Nodules (n = 49)	No. of Benign Nodules (n = 58)
≥25 Wash-in, 5–31 washout (type I)	46	6
<25 Wash-in (type II)	0	27
≥25 Wash-in with persistent enhancement (type III)	1	14
≥25 Wash-in, >31 washout (type IV)	2	11

TABLE 5
Patterns of Nodule Enhancement according to Histologic Diagnosis

Diagnosis	Type I (n = 52)	Type II (n = 27)	Type III (n = 15)	Type IV (n = 13)
Adenocarcinoma (n = 33)	30	0	1	2
Non–small cell lung cancer (n = 8)	8	0	0	0
Squamous cell carcinoma (n = 3)	3	0	0	0
Small cell carcinoma (n = 1)	1	0	0	0
Bronchioloalveolar cell carcinoma (n = 1)	1	0	0	0
Metastatic carcinoma (n = 1)	1	0	0	0
Pleomorphic carcinoma (n = 1)	1	0	0	0
Carcinoid tumor (n = 1)	1	0	0	0
Tuberculosis (n = 2)	0	2	0	0
Hamartoma (n = 8)	0	4	3	1
Focal pneumonia without specific microorganism (n = 4)	3	0	1	0
Sclerosing hemangioma (n = 1)	0	0	0	1
Pulmonary infiltration of eosinophilia (n = 2)	0	0	2	0
Progressive massive fibrosis (n = 1)	0	0	1	0
Leiomyoma (n = 1)	0	0	0	1
Anthracofibrotic nodule (n = 1)	1	0	0	0
Aspergilloma (n = 1)	0	1	0	0
Benignancy with imaging (n = 37)	2	20	7	8

Note.—Data are numbers of nodules that showed type I (≥25 HU wash-in, 5–31 HU washout), type II (<25 HU wash-in), type III (≥25 HU wash-in with persistent enhancement), or type IV (≥25 HU wash-in, >31 HU washout) enhancement.

odds ratio, 13.8)—was useful for the diagnosis of a malignant nodule from the multivariate analysis controlling the effect of other diagnostic factors.

DISCUSSION

In general, malignant nodules tend to enhance substantially more than benign nodules (1,2,4–7). Yamashita et al (19) reported that a maximum attenuation of 20–60 HU appears to be a good predictor of malignancy. A report by Swensen et al (6) in 2000 is also noteworthy, in that the authors reported a threshold value of 15 HU produced a sensitivity of 98%, a specificity of 58%, and an accuracy of 77% for malignant nodules. Cutoff values for the differentiation between benign and malignant nodules have since been set at 15 or 20 HU. However, in a dynamic study with multi–detector row CT (4), higher peak enhancement was obtained in comparison with that in previous studies performed with conventional or single–detector row helical CT, and thus higher attenuation cutoff values could be used for differentiation. Actually, with a cutoff value of 30 HU of net enhancement, overall diagnostic accuracy (sensitivity of 99%, specificity of 54%, positive predictive value of 71%, negative predictive value of 97%, and an accuracy of 78%) was similar to that in previous studies performed by using single–detector row spiral CT. However, all of these previous dynamic CT studies (1,2,4,6) were focused on the early phase of dynamic CT scanning, and results showed low specificities that ranged from 54% to 77%. Moreover, early-phase dynamic CT did not help differentiate malignant nodules from active granulomas or benign vascular tumors.

Transport of contrast medium through the lung involves the intravascular and interstitial spaces (20). The vascular supply of most malignant pulmonary nodules is from the bronchial arterial system (20,21). Washout from the intravascular space in malignant nodules takes place via the bronchial veins. A large interstitial space has been found in some human and experimental malignant tumors (22). Most important, in the washout phase from the interstitial space, a near absence or substantial reduction of lymphatic flow is noted in malignant tumors (20). The retarded flow in the intravascular and interstitial spaces would contribute to the retention of contrast medium in malignant nodules. In most inflammatory pulmonary processes, because of diffuse thrombosis at the arterioles of the pulmonary circulation, the vascular supply is actually from the bronchial arteries, which are shown to increase in size and number (23). Outflow of contrast medium (washout) through the intravascular space in an inflammatory situation is taking place through relatively straight vessels with a normal configuration, and

washout of contrast medium from the interstitial space is accelerated by active lymphatic flow (24). In the inflammatory nodules, the time-attenuation curve declines after reaching peak height because of normal washout (7). In malignant nodules, the curve changes little after reaching peak height because of the retarded flow in the washout phase.

In our study, one malignant nodule (an adenocarcinoma) and 14 benign nodules showed persistent enhancement without washout. We speculate that persistent enhancement without washout on dynamic contrast-enhanced CT scans may be related to the amount and degree of fibrosis (25–27). Delayed uptake of contrast medium may be attributed to redistribution of it. Namely, in the early phase, the well-vascularized tumor cell zones show contrast enhancement; once contrast medium moves into abundant fibrous tissue with scanty blood supply in the late phase, it remains there, showing the fibrotic portion of the nodule for a long time without washout.

To the best of our knowledge, no evaluation of the accuracy of a protocol based on the combination of these two properties (wash-in and washout characteristics) has been reported. In our study, the threshold value, wash-in enhancement of 25 HU or more, was reached by all malignant nodules. However, by analyzing the wash-in phase only, the false-positive rate was 52% (30 of 58 benign nodules). The use of the washout characteristics of dynamic enhancement allowed us to correctly diagnose 24 of 30 benign nodules and to reduce the false-positive rate.

In our study, in 45 of 49 malignant nodules the peak level of enhancement occurred within 5 minutes of initiating the injection of contrast material. However, in four malignant nodules the peak level of enhancement occurred more than 5 minutes after injection. The mean time to peak enhancement in malignant nodules was 3.2 minutes. In a previous study (5), the peak level of enhancement in most malignant nodules (96%) occurred during the first 2 minutes after initiating the injection. Therefore, the authors of that study pointed out the diagnostic importance of attenuation measurements over the first 2 minutes of dynamic CT. However, in our study, only 57% of the malignant nodules showed peak enhancement during the first 2 minutes after injection was initiated. Yamashita et al (19) observed that some lung carcinomas reached peak enhancement late, at 5 minutes. This finding reflects the fact that some lung carcinomas have a wide extravascular fluid pool. Contrast enhancement values obtained at CT are a summation of the intra- and extravascular concentrations of contrast medium. The distribution of contrast material approaches a balance at 5 minutes after injection, being directly related to the volume of the extracellular space, with more than 80% of the contrast medium remaining outside blood vessels (28).

The real clinical value of dynamic contrast-enhanced CT for the differentiation of malignant and benign nodules may be in the evaluation of radiologically indeterminate small nodules, in which it is difficult to perform biopsy successfully. In our study, 36% of nodules (39 of 107) were less than 15 mm in diameter. In a previous study by Swensen et al (2), 44% of nodules (47 of 107) were less than 15 mm in diameter.

In our study, the measured total organ dose at thin-section, dynamic, and staging CT ranged from 98 to 115 mGy at the nodule sites. This dose at nodule location is about five times larger than that used for single–detector row helical CT (18–19 mGy with 1–10-mm collimation, 120 kVp, 300 mAs) (29) and is about two and half times larger than that used for standard helical multi–detector row CT (39–40 mGy) performed at our institu-

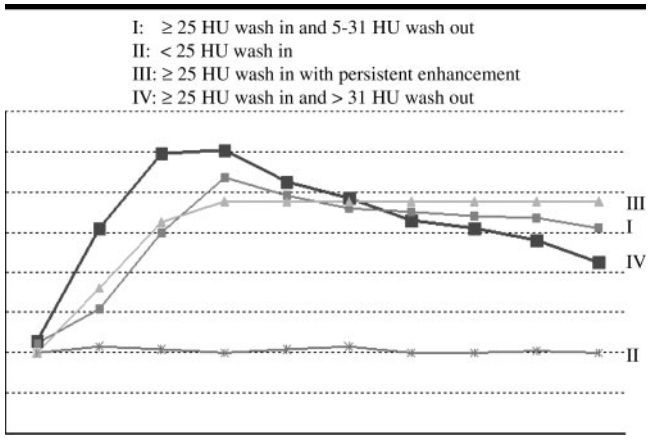

Figure 1. Graph of four different types of time-attenuation curve of nodule hemodynamics in consideration of both wash-in and washout phases of dynamic CT.

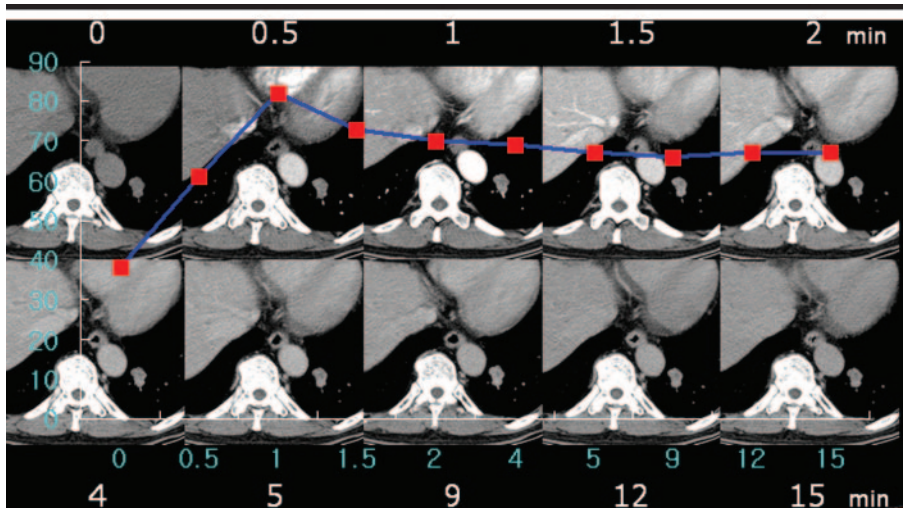

Figure 2. CT scans of adenocarcinoma with type I enhancement (≥25 HU wash-in, 5–31 HU washout) in a 63-year-old man. Serial transverse images obtained through a nodule in the left lower lobe for 15 minutes enable one to plot the dynamic enhancement curve for the nodule. Peak enhancement is 82 HU; net enhancement, 44 HU; absolute loss of enhancement (washout), 15 HU; and time to peak enhancement, 1 minute.

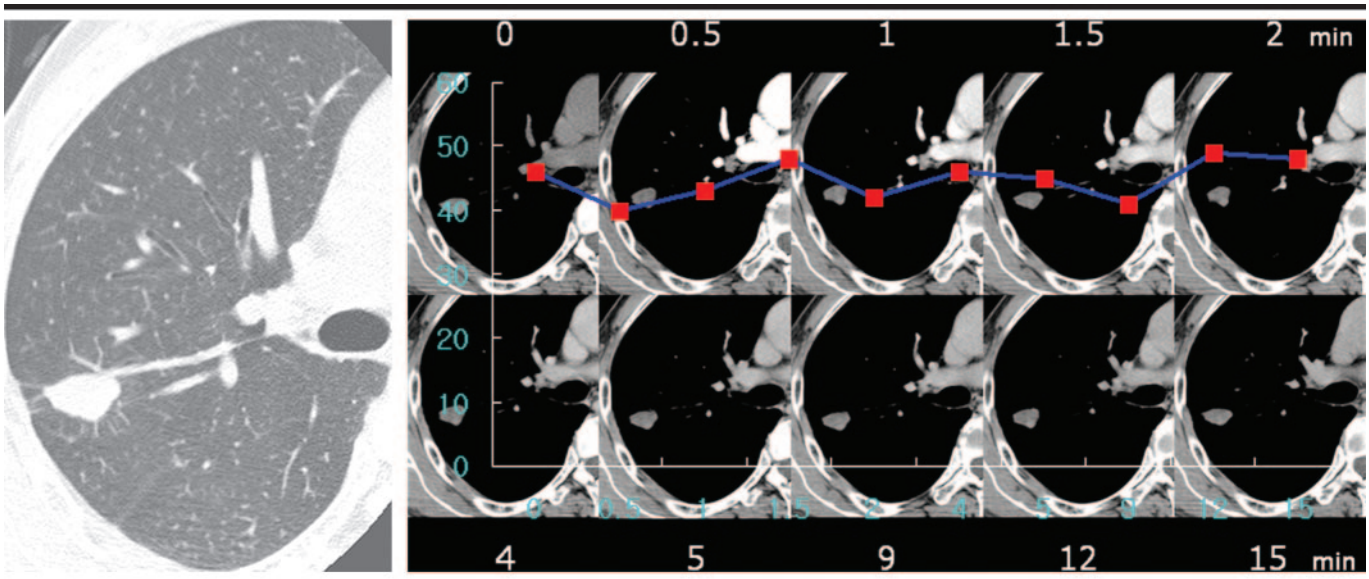

a. b.

Figure 3. CT scans of tuberculoma with type II enhancement (<25 HU wash-in) in a 58-year-old man. **(a)** Transverse thin-section (2.5-mm collimation) scan obtained with lung window at the level of the right main bronchus shows 21-mm nodule with lobulated and spiculated margin in the right upper lobe. **(b)** Serial images with dynamic enhancement curve for the nodule. Peak enhancement is 49 HU; net enhancement, 3 HU; and absolute loss of enhancement (washout), 1 HU.

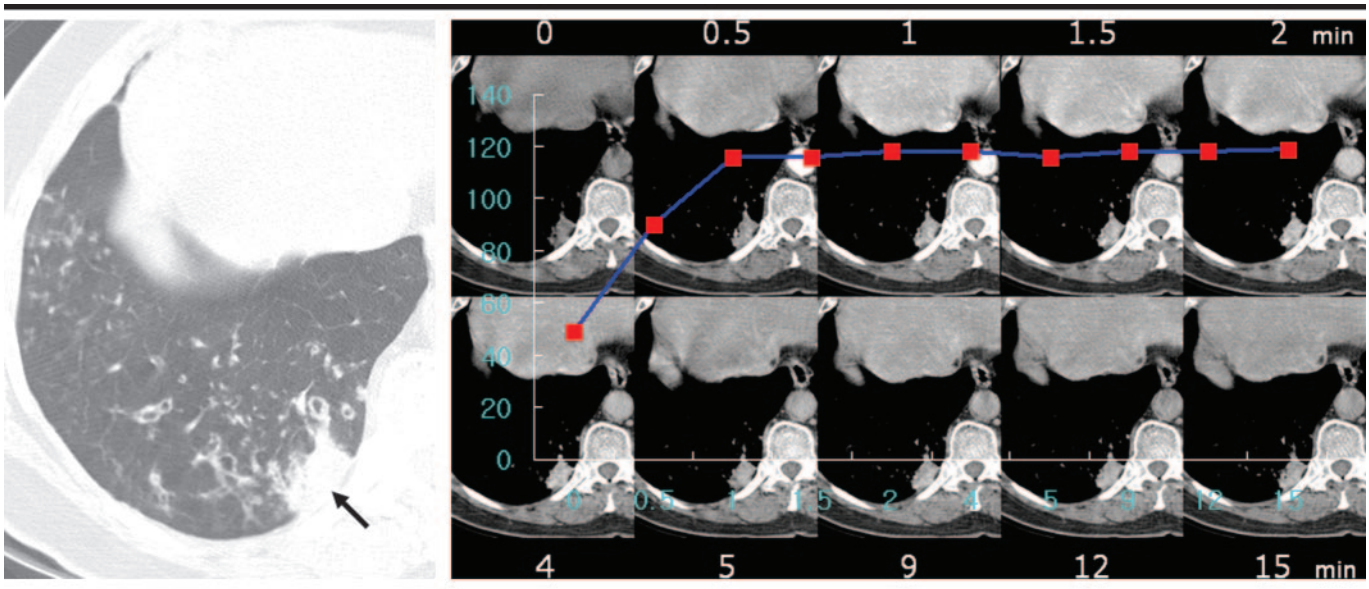

a. b.

Figure 4. CT scans of organizing pneumonia (focal pneumonia without specific microorganism) with type III enhancement (≥25 HU wash-in with persistent enhancement) in a 58-year-old woman. **(a)** Transverse thin-section (2.5-mm collimation) scan obtained with lung window at the level of the hepatic dome shows 14-mm nodule (arrow) in right lower lobe. Bronchiectasis is also seen in both lower lobes. **(b)** Serial images with dynamic enhancement curve for the nodule. Peak enhancement is 118 HU; net enhancement, 69 HU. This nodule showed persistent enhancement without absolute loss of enhancement.

tion. However, this organ dose applies only to the thin (3 cm in length along the z-axis) bandlike area of the nodule location. An increased band of organ dose at a nodule location in women may often be in the breast tissue, and, therefore, this technique may not be appropriate for women with a low pretest probability of malignancy or even to young women when a T1N0 lung cancer is suspected. The dose (35–40 mGy) in other areas is similar to or slightly lower than that with our standard helical CT technique. We obtained a total of 10 series of images at various times for 15 minutes. Because images obtained at certain time points may provide little information, truncation of the protocol (not obtaining an image series at, for example, 9 minutes and 12 minutes) might have contributed to the mitigation of radiation dose.

There were several limitations to our study. First, pathologic proof was not obtained for all benign nodules. However, although the follow-up period was somewhat short (average, 11.7 months), follow-up CT scans helped to diagnose benignancy by showing no growth or a decrease in the size of nodules.

Second, we did not attempt to standardize the injection rate or volume of contrast material according to the cardiac output for each patient, and we did not routinely use CT software techniques (SmartPrep; GE Medical Systems) to time the initiation of scanning in consideration of peak enhancement. For a more uniform and standardized delivery of contrast medium while reducing the total amount of contrast medium injected, saline chaser can be administered with a double-barrel injector (30). In addition, we did not standardize the volume of contrast material according to patient weight. However, these techniques are either variably used or not used in clinical practice, and, therefore, we believe that our results are likely to reflect those in the clinical situation.

Third, no pathophysiologic data or proof is presented to explain the washout characteristics of benign and malignant nodules. However, angioarchitectural differences, such as the integrity of cellular membranes or the extracellular space volumes, might be present in benign and malignant nodules (31,32). It should also be pointed out that placing the regions of interest accurately on nodules is important when attempting to measure their attenuation values on CT scans. Inadequate placement of regions of interest on nodules leads to erroneous attenuation values, which can lead to false wash-in and washout enhancement calculations.

Fourth, our study may contain a selection bias. We excluded 10 patients with no histologic diagnosis or follow-up images. However, most of the excluded patients had no follow-up study or study of less than 6 months, and some patients were excluded because they refused to undergo surgery or biopsy. Neither surgical criteria nor dynamic CT results precluded our including patients in this study.

Fifth, we arbitrarily chose a 15-minute delay, which we believe allowed enough time for the washout of contrast material from a pulmonary nodule, given practical time constraints. Although this modality did not provide a perfect test, the application of attenuation threshold values of wash-in and washout resulted in the differentiation of benign and malignant nodules with high sensitivity and specificity.

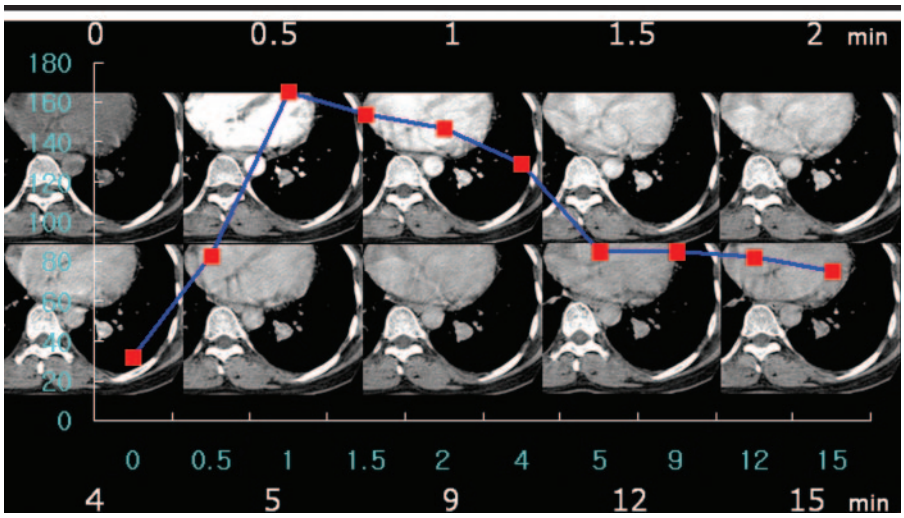

Figure 5. CT scans of leiomyoma with type IV enhancement (≥25 HU wash-in, >31 HU washout) in a 45-year-old woman. Serial images with dynamic enhancement curve for the left lower lobe nodule show peak enhancement is 165 HU; net enhancement, 133 HU; absolute loss of enhancement (washout), 90 HU; and time to peak enhancement, 1 minute.

Sixth, the threshold values (≥25 HU of net enhancement and 5–31 HU of washout for malignant nodules) chosen in this study were derived retrospectively from the data and were then applied to get diagnostic characteristics. Consequently, the high sensitivity, specificity, and accuracy values may not be the same in future studies.

Finally, we used fixed-form CT imaging (2.5-mm collimation) and reconstruction (2.5-mm) parameters for covering 3 cm along the z-axis. If we acquired thinner (eg, 1.0-mm-reconstruction) images, evaluation of smaller nodules (<7 mm in diameter) on dynamic images would have been feasible.

In conclusion, malignant nodules can be characterized by means of a net enhancement of 25 HU or more and a washout of 5–31 HU. Benign nodules can be characterized by means of a net enhancement of less than 25 HU, a net enhancement of 25 HU or more in combination with a washout enhancement of 31 HU or more, or a net enhancement of 25 HU or more and persistent enhancement without washout. The evaluation of solitary pulmonary nodules by analyzing combined wash-in and washout characteristics at dynamic multi–detector row CT proved useful for differentiating between benign and malignant nodules. However, our study is still a category of work in progress. Further multi-institutional studies, especially those on radiation dose reduction by means of truncating image acquisition sequences and those on imaging parameters (eg, different machines, section thickness, or pitch) are needed.

References

1. Swensen SJ, Brown LR, Colby TV, Weaver AL. Pulmonary nodules: CT evaluation of enhancement with iodinated contrast material. Radiology 1995;194:393–398.
2. Swensen SJ, Brown LR, Colby TV, Weaver AL, Midthun DE. Lung nodule enhancement at CT: prospective findings. Radiology 1996;201:447–455.
3. Yamashita K, Matsunobe S, Takahashi R, et al. Small peripheral lung carcinoma evaluated with incremental dynamic CT: radiologic-pathologic correlation. Radiology 1995;196:401–408.
4. Yi CA, Lee KS, Kim EA, et al. Solitary pulmonary nodules: dynamic enhanced multi–detector row CT study and comparison with vascular endothelial growth factor and microvessel density. Radiology 2004;233:191–199.
5. Swensen SJ, Morin RL, Schueler BA, et al. Solitary pulmonary nodule: CT evaluation of enhancement with iodinated contrast material—a preliminary report. Radiology 1992;182:343–347.
6. Swensen SJ, Viggiano RW, Midthun DE, et al. Lung nodule enhancement at CT: multicenter study. Radiology 2000;214:73–80.
7. Zhang M, Kono M. Solitary pulmonary nodules: evaluation of blood flow patterns with dynamic CT. Radiology 1997;205:471–478.
8. Mack MJ, Hazelrigg SR, Landreneau RJ, Acuff TE. Thoracoscopy for the diagnosis of the indeterminate solitary pulmonary nodule. Ann Thorac Surg 1993;56:825–830.
9. Siegelman SS, Zerhouni EA, Leo FP, Khouri NF, Stitik FP. CT of the solitary pulmonary nodule. AJR Am J Roentgenol 1980;135:1–13.

10. Bernard A. Resection of pulmonary nodules using video-assisted thoracic surgery. The Thorax Group. Ann Thorac Surg 1996; 61:202–204.
11. Keagy BA, Starek PJ, Murray GF, Battaglini JW, Lores ME, Wilcox BR. Major pulmonary resection for suspected but unconfirmed malignancy. Ann Thorac Surg 1984;38:314–316.
12. St. Anthony's DRG guidebook. Reston, Va: St. Anthony's Publishing, 1996.
13. Korobkin M, Brodeur FJ, Francis IR, Quint LE, Dunnick NR, Goodsitt M. Delayed enhanced CT for differentiation of benign from malignant adrenal masses. Radiology 1996;200:737–742.
14. Boland GW, Hahn PF, Pena C, Mueller PR. Adrenal masses: characterization with delayed contrast-enhanced CT. Radiology 1997;202:693–696.
15. Szolar DH, Kammerhuber FH. Adrenal adenomas and nonadenomas: assessment of washout at delayed contrast-enhanced CT. Radiology 1998;207:369–375.
16. Pena CS, Boland GW, Hahn PF, Lee MJ, Mueller PR. Characterization of indeterminate (lipid-poor) adrenal masses: use of washout characteristics at contrast-enhanced CT. Radiology 2000;217:798–802.
17. Caoili EM, Korobkin M, Francis IR, et al. Adrenal masses: characterization with combined unenhanced and delayed enhanced CT. Radiology 2002;222:629–633.
18. Jung KJ, Lee KS, Kim SY, Kim TS, Pyeun YS, Lee JY. Low-dose, volumetric helical CT: image quality, radiation dose, and usefulness for evaluation of bronchiectasis. Invest Radiol 2000;35:557–563.
19. Yamashita K, Matsunobe S, Tsuda T, et al. Solitary pulmonary nodule: preliminary study of evaluation with incremental dynamic CT. Radiology 1995;194:399–405.
20. Littleton JT, Durizch ML, Moeller G, Herbert DE. Pulmonary masses: contrast enhancement. Radiology 1990;177:861–871.
21. Milne EN. Circulation of primary and metastatic pulmonary neoplasms: a postmortem microarteriographic study. Am J Roentgenol Radium Ther Nucl Med 1967; 100:603–619.
22. Peterson HI. Vascular and extravascular spaces in tumors: tumor vascular permeability. In: Peterson HI, ed. Tumor blood circulation: angiogenesis, vascular morphology and blood flow of experimental and human tumors. Boca Raton, Fla: CRC, 1979; 77–86.
23. Deffebach ME, Charan NB, Lakshminarayan S, Butler J. The bronchial circulation: small, but a vital attribute of the lung. Am Rev Respir Dis 1987;135:463–481.
24. Dewan NA, Gupta NC, Redepenning LS, Phalen JJ, Frick MP. Diagnostic efficacy of PET-FDG imaging in solitary pulmonary nodules: potential role in evaluation and management. Chest 1993;104:997–1002.
25. Muramatsu Y, Takayasu K, Moriyama N, et al. Peripheral low-density area of hepatic tumors: CT-pathological correlation. Radiology 1986;160:49–52.
26. Takayasu K, Ikeya S, Mukai K, Muramatsu Y, Makuuchi M, Hasegawa H. CT of cholangiocarcinoma: late contrast enhancement in six patients. AJR Am J Roentgenol 1990;154:1203–1206.
27. Furukawa H, Takayasu K, Mukai K, et al. Late contrast-enhanced CT for small pancreatic carcinoma: delayed enhanced area on CT with histopathological correlation. Hepatogastroenterology 1996;43:1230–1237.
28. Naidich DP, Zerhouni EA, Siegelman SS. Principles and techniques of chest computed tomography. In: Naidich DP, Zerhouni EA, Siegelman SS, eds. Computed tomography of the thorax. New York, NY: Raven, 1984;9–12.
29. McNitt-Gray MF. AAPM/RSNA physics tutorial for residents: topics in CT—radiation dose in CT. RadioGraphics 2002;22:1541–1553.
30. Dorio PJ, Lee FT, Henseler KP, et al. Using a saline chaser to decrease contrast media in abdominal CT. AJR Am J Roentgenol 2003;180:929–934.
31. Kormano M, Dean PB. Extravascular contrast material: the major component of contrast enhancement. Radiology 1976; 121:379–382.
32. Newhouse JH, Murphy RX Jr. Tissue distribution of soluble contrast: effect of dose variation and changes with time. AJR Am J Roentgenol 1981;136:463–467.